Tuijin Jishu/Journal of Propulsion Technology
ISSN: 1001-4055
Vol. 45 No. 3 (2024)

A Numerical Study on 3D Finite Element Model of Steel-Concrete Composite Beams with Trapezoidal Steel Decking

Avinash Bhakta[1], Dr. Sudipta K. Mishra[2]

[1]PhD Scholar, Department of Civil Engineering, G. D. Goenka University, Gurugram, Haryana, India

[2]Associate Professor, Department of Civil Engineering, G. D. Goenka University, Gurugram, Haryana, India

Abstract

Modern construction frequently employs steel-concrete composite beams (CBs), welding headed shear stud connections utilising profiled steel sheeting (PSS) to guarantee full or partial composite action across the beam and composite slab. Our study focuses on CBs having trapezoidal steel decking. CBs fail in several ways due to complicated component interactions. Finite element (FE) analysis can grasp the fundamental conduct of these beams. So, previous FE models simplified complex interactions, like those between shear studs and concrete, by making assumptions. Therefore, some failure modes remain unaccounted for by these FE models, and the forces acting on the studs and also PSS remain unquantified. This work aims to create a thorough 3D FE model for CBs having trapezoidal steel decking. The model simulates shear stud and PSS fractures, concrete tensile and compressive damage, and other component interactions. The full-extent load-deformation curves for the CBs and the shear force-slip (SFS) connection for the embedded shear studs are exactly what our FE model says they will be. The FE model accurately and reliably predicts the actions of steel-concrete CBs having trapezoidal steel decking, matching a vast array of test data from the literature.

Keywords: *Composite beams, finite element modeling, trapezoidal steel decking, analytical*

Introduction

In the construction of steel-framed buildings, there has been extensive use of steel-concrete CBs having profiled steel sheets. For full-scale testing, such CBs necessitate elaborate, time-consuming, and expansive testing facilities **[1, 2].** Consequently, conducting experimental investigations into the effects of different parameters is a highly costly endeavour. Finite element (FE) modelling, as an alternative method, can help us grasp the basic conduct of CBs. Composite beams, particularly those made of PSS, can be notoriously difficult to model owing to steel and concrete's nonlinear behavior, the sheer number of contact surfaces, and the corrugated shape of the steel sheeting.

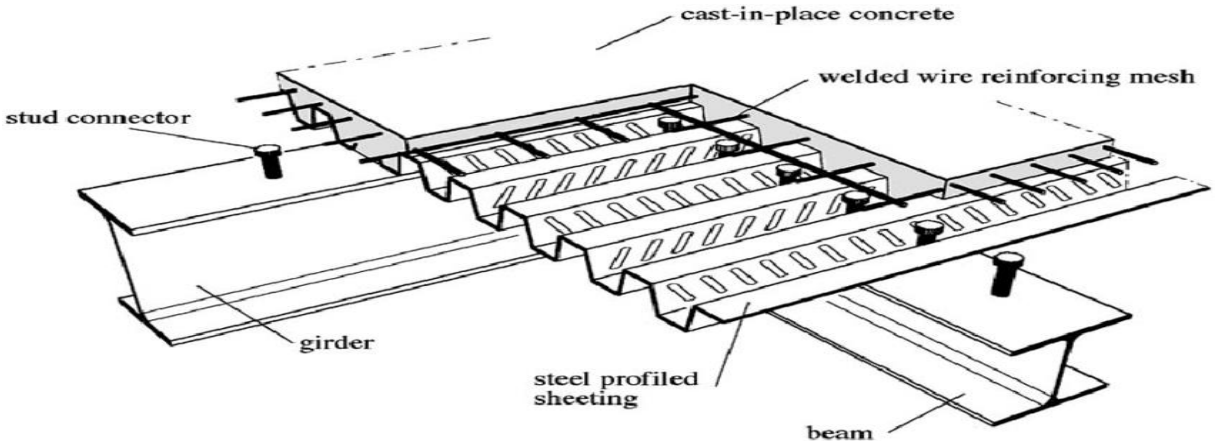

Figure 1.1Composite floor with steel profiled sheeting Crisinel and Marimon,(2004)[18]

A lot of work has gone into creating finite element models for CBs **[3, 4]** and push test specimens **[5, 6]** according to Eurocode[1] standards so that we can constantly gauge the relative slide between the steel and concrete while we load them. The shear studs inside CBs were typically represented as "embedded constraints" **[7, 8]** or "connector elements" in order to avoid numerical convergence problems and/or the high computational cost. By utilising "embedded constraints" to fully embed a stud in the concrete, the relative movement across the stud along with concrete is prohibited, thereby concealing the stud's actual slip conduct. At the same time, this streamlined approach may miss any stud fractures. Some studies dealt with this limitation by just embedding a portion of the stud inside the concrete **[9, 10, 11].** Nevertheless, the embedding interaction that has been defined is not entirely precise. However, when "connector elements" are included, it is necessary to establish the studs' SFS relationship by utilising a simplified model or data derived from push tests. In order to simulate CBs, for instance, several researchers have relied on the standard SFS model created by **Tong et al. (2020) [10].** A limitation of this model is the absence of a descending branch in its SFS curve, which fails to capture the true SFS relationship of shear studs at full-extent. Improving this requires a thorough understanding of and accurate incorporation of the model of the impacts of concrete failure along with shear stud fracture. Furthermore, shear stud performance in push tests might not be indicative of how shear studs inside CBs actually behave. This is due to the fact that the push test does not involve beam curvature or normal force due to floor loading **[13, 14].** Results from full-scale CB testing compared to companion push tests have verified this **[15, 16].**

Compared to push testing, CB tests showed that shear studs were more ductile. For the same reasons, forecasting the conduct of CBs using FE models that use either the "embedment interaction" across the stud alongside concrete or "connector elements" to reflect shear stud performance is not without its limits **[17, 18].**

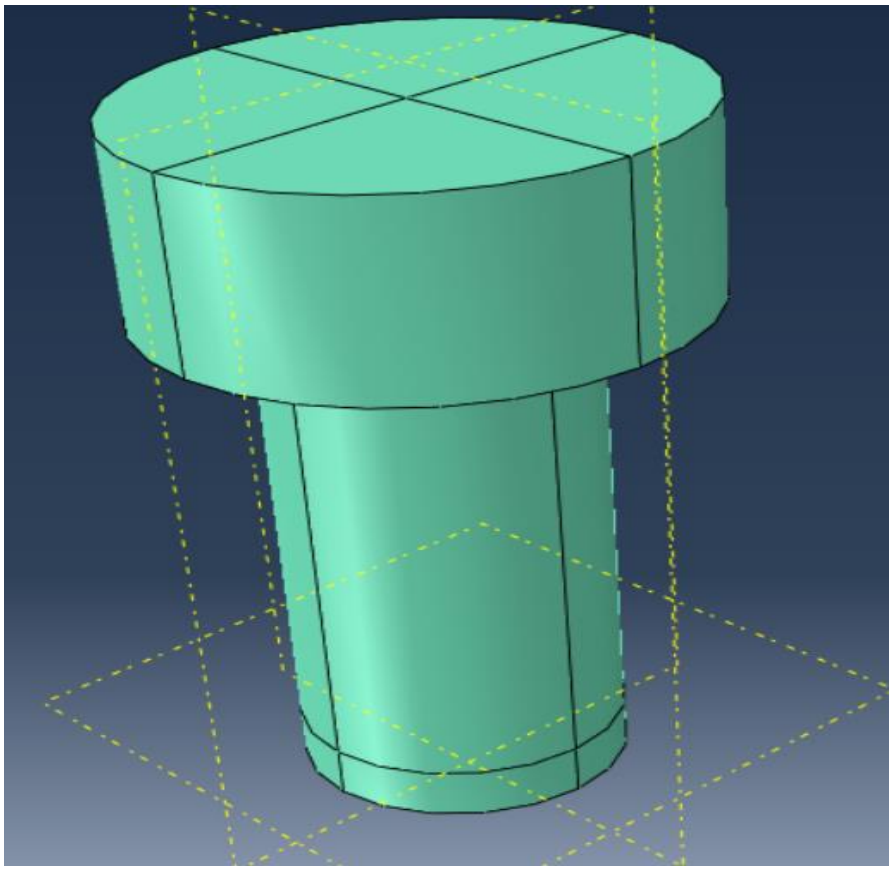

Figure 1.2 Typical shear studs Tong et al. (2020) [10].

[1] European Committee for Standardization (CEN), Design of composite steel and concrete structures - part 1-1: general rules and rules for buildings, EN 1994-1-1 Eurocode 4, Brussels, 2004

Simplified models including shear studs' realistic SFS conduct in CBs are advantageous in structural analysis and design. Having a complete grasp of the intricate interplay between various components in CBs is crucial for developing an accurate SFS model. A precise and versatile 3D FE model might be developed to solve this problem; this is the main topic of the study by **Lin, Lei, and Jian (2021) [14].** The computed FE models allow for the quantitative determination of the shear forces possessed by the studs and the axial forces possessed by the PSS. CBs having PSS will have FE model that considers the realistic interaction of various components in order to capture various failure modes, like stud shear, and concrete crushing, and steel beam, along with rib shear failures **[19, 20].** The concrete within the PSS might break due to the internal longitudinal shear force, which is known as rib shear failure. Various test results published in the literature will confirm the accuracy of the full-extent load-deformation curves of CBs and the slip conduct of shear studs **[21, 22].**

Research Gap

Although there have been improvements in the modeling of steel-concrete composite beams (CBs), there are still substantial deficiencies in accurately forecasting the intricate interactions between the different components, especially with regards to trapezoidal steel decking. Conventional finite element (FE) models frequently simplify or neglect important interactions, such as the interactions between shear studs and concrete, or the impacts of local buckling in steel beams. These simplifications may result in differences between the predicted and observed performance, particularly when there are different loading conditions. This study overcomes these constraints by creating a detailed 3D finite element model that accurately represents the complex behaviors and failure modes of composite beams with trapezoidal steel decking. This work is unique because it provides a thorough analysis of how shear studs behave and how concrete is damaged. It also takes into account the realistic interactions between different components, resulting in a more precise prediction of the performance and failure modes of composite beams.

Aims and Objectives

This study aims to create and evaluate finite element models of steel-concrete CBs that incorporate trapezoidal steel decking. Comprehensive information regarding the connection components, parameters, material specifications, loadings, and boundary conditions was provided for both models. The experimental and numerical analysis of these components is also considered.

The Research Objectives (RO) of this study are as follows

RO1. To create a 3D FE model that can predict all CB failure modes.

RO2. To compare the numerical outcomes gotten from the offered 3D FE model from that of the experimental results from the literature.

Finite element modelling

A typical FE model has five components: steel beam, and shear studs, and PSS, and concrete slab, along with reinforcement bars (Fig. 1.1(a)). Stiffeners soldered to a steel beam looking to prevent/delay web or flange buckling were simulated to match the test condition. Single-span beams are utilised to test CB capacity under positive or even negative moment, depending on loading direction. In Fig. 1.1(c), two concentrated loads are then applied straight downward to test the beam right under +ve moment, a frequent condition **[23]**. To boost computational efficiency, a half-symmetry model was created for a positive-moment single-span beam. However, comprehensive models were created to simulate CB deformation, including local buckling of steel I-section flanges and webs, for single-span beams right under -ve moment or even continuous beams.

All components except PSS along with reinforcement bars were then simulated utilising C3D8R solid elements. PSS was replicated utilising shell elements (S4R) and reinforcing bars with T3D2). Many Poisson's ratio tests have been done on steel and concrete. Poisson's ratios for steel alonside concrete are generally accepted as 0.3 alongside 0.2 **[24, 25].** Thus, this analysis uses those values.

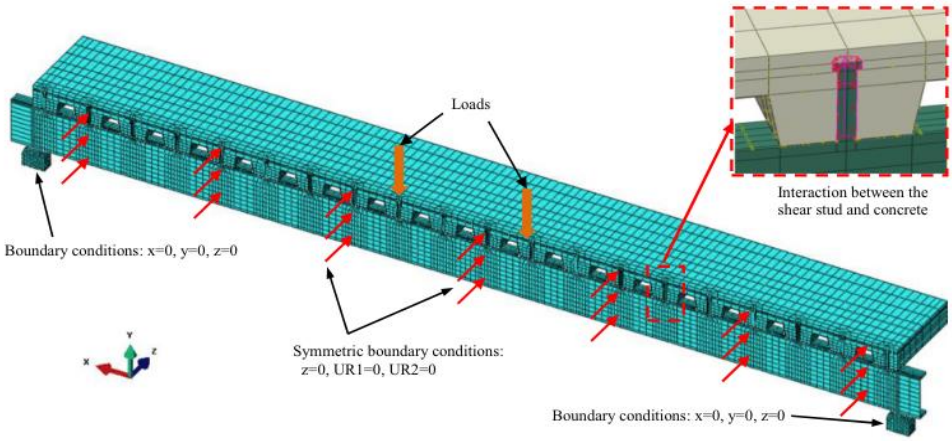

(a) Typical FE model

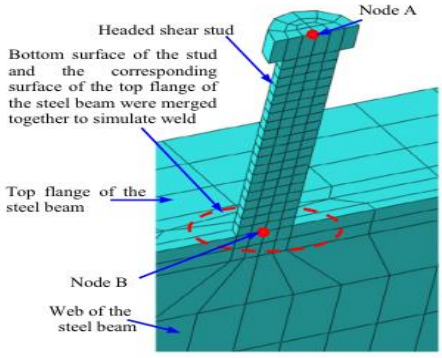

(b) Simulation of shear studs

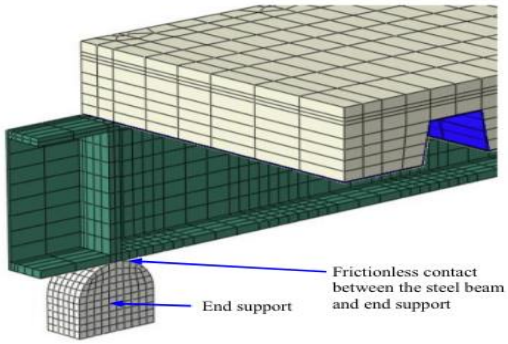

(c) Boundary conditions

Figure 1.3 FE model of a typical CB under positive moment

Methodology

In this investigation, the conduct of steel-concrete CBs having trapezoidal steel decking was predicted through the progression of comprehensive 3D FE models utilising ABAQUS version 6.14**[23]**. The steel beam, and shear studs, PSS, concrete slab, along with reinforcement bars are the five main parts of a standard FE model. Additionally, stiffeners were simulated for beams that had them in order to prevent local buckling. Solid elements were utilised to simulate the steel beam (C3D8R). The web was divided into 16 elements having max. size - 25 mm for negative moment beams and at least 8 elements for positive moment beams, having max. size - 40 mm. Also, the flanges were divided into ten elements, each no larger than 40 mm. The elements used to mesh the shear studs were either 4 mm or Ds/4, depending on which was smaller. Shell elements (S4R) were used to represent the PSS, and 100 mm element size two-node truss elements (T3D2) were used to simulate the reinforcement bars. The element sizes of the concrete slab ranged 40 - 150 mm in other locations and from 15 to 30 mm in rib sections. For contact surfaces, surface-to-surface interactions were defined. Based on sensitivity research, the friction coefficient across profiled steel sheets and concrete was determined to be 0.01. The contact across the PSS and the steel beam, along with the concrete and shear studs, both used the same friction coefficient.

Self-weight was taken into account in the examination of the hinged and roller-supported beams that the model simulated. In the initial phase, the self-weight was applied and then carried forward as a continuous load in subsequent steps, together with any further imposed weights. It ranged from 10 to 25% of the entire load capacity.

The steel beams were materially modelled using an elastic-plastic stress-strain model having strain hardening. Similar to the steel beams, the steel reinforcement was modelled with an initial elasticity modulus of 0.03Es at the beginning of the strain-hardening process. An elastic-perfectly plastic model with fracture criteria was utilised to model the PSS, with a failure strain (εf) of 4.5%. The shear studs used updated strains (εu1 = 25εy, εf = 80εy, and εu2 = 90εy) and followed a full-extent stress-strain model with a defined failure stage.

The Concrete Damaged Plasticity (CDP) model was utilised to simulate tensile cracking and potential crushing failure in the concrete. ACI 318 was utilised to determine elasticity modulus E_c, which was found to be $4700\sqrt{f_c'}$. The flow potential eccentricity (e) was set to 0.1 as the default value, and the dilation angle (ψ) was given a value of 30°. The default values of 1.16 and 0.667 were assigned to the parameters $f_b//f_c^a$ and K_c respectively. In order to resolve issues with convergence, 0.0001 was chosen as the viscosity parameter

Results and Discussion

Failure Modes Prediction

The proposed 3D FE model was made to foresee various failure modes in CBs, counting shear stud fracture, and concrete crushing, and steel beam, along with rib shear failures. The model's effectiveness in predicting these failure modes was validated against experimental data from 22 CB specimens reported in the literature.

Shear Stud Fracture

RO1. To create a 3D FE model that can predict all CB failure modes.

The fracture of shear studs was successfully predicted in specimens having a degree of shear connection (η) approx. 0.5 or even less, causing strength deterioration. So, Table 1 presents the specimens that exhibited shear stud fracture, along with the comparison across predicted along with measured ultimate loads.

Table 1: Comparison of Predicted and Measured Ultimate Loads for Shear Stud Fracture

Specimen	η	P_{ue} (kN)	P_{uc} (kN)	P_{ue} (kN)/Puc (kN)
SB1	0.5	210	205	1.024
SB8	0.5	195	190	1.026

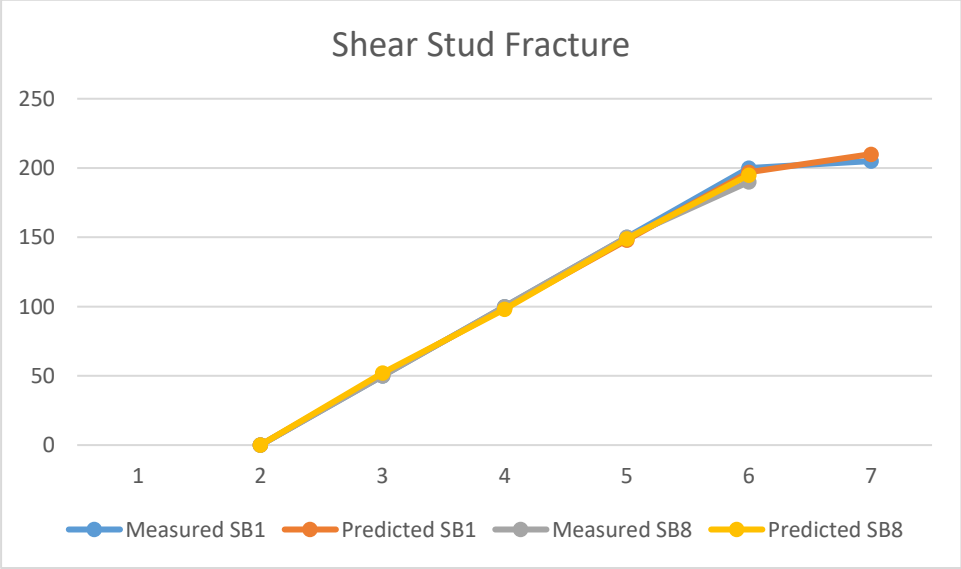

Figure 1.2: Predicted vs. Measured P-Δ Curves for Specimens SB1 and SB8 (Shear Stud Fracture)

Concrete Crushing Failure

Concrete crushing failure was predicted in specimens with high degrees of shear connection and compact beam sections. The compressive damage variable (DAMAGEC) in ABAQUS was utilised to signify the concrete slab's crushing failure.

Table 2: Concrete Crushing Failure Prediction

Specimen	η	P_{ue} (kN)	P_{uc} (kN)	P_{ue} (kN)/Puc (kN)
SB2	0.666	220	200	1.100
SB3	0.666	225	210	1.071

Steel Beam Failure

Steel beam failure under positive and negative moments was captured by the model, including local buckling of the web along with bottom flange.

Table 3: Steel Beam Failure Prediction

Specimen	Moment Type	P_{ue} (kN)	P_{uc} (kN)	P_{ue} (kN)/Puc (kN)
CB1	Negative	230	220	1.045
SB6	Negative	240	228	1.053

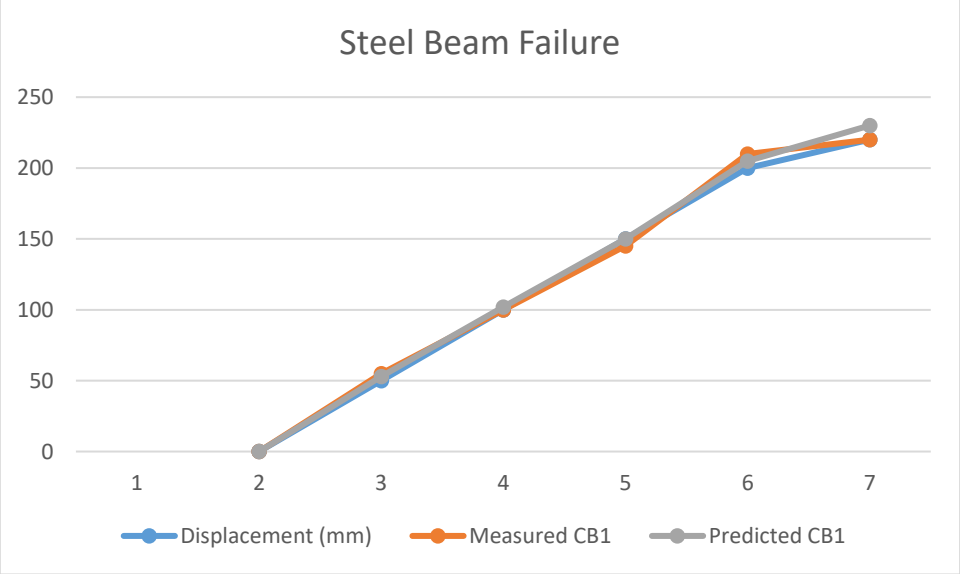

Figure 1.4: Predicted vs. Measured P-Δ Curves for Specimen CB1 (Steel Beam Failure)

Rib Shear Failure

Rib shear failure was observed in specimens with small trough and slab widths. The predicted tensile damage variable (DAMAGET) was utilised to indicate shear cracks in the concrete

Table 4: Rib Shear Failure Prediction

Specimen	Trough Width (mm)	Slab Width (mm)	P_{ue} (kN)	P_{uc} (kN)	P_{ue} (kN)/Puc (kN)
SB4	70	1000	210	200	1.050
SB5	70	1000	215	205	1.049
JB-1	1220	1220	250	240	1.042

Comparison of Numerical and Experimental Results

The cogency of the suggested FE model was confirmed by likening it to experimental data, revealing a strong correlation across the predicted along wihth measured ultimate loads. The Pue/Puc ratio had mean - 1.012 and a std. dev. - 0.052, suggesting a good level of prediction accuracy. The deviation between the predicted and actual ultimate load did not exceed ±10% for all specimens, barring Beam 2 examined by Hicks.

Table 5: Overall Comparison of Predicted and Measured Ultimate Loads

Specimen	P_{ue} (kN)	P_{uc} (kN)	P_{ue} (kN)/Puc (kN)
Beam 1	260	250	1.040
Beam 2	270	245	1.102
CB1	230	220	1.045
CB2	240	228	1.053
SB1	210	205	1.024
SB2	220	200	1.100
SB3	225	210	1.071

Load-Deflection Curves

The predicted load-deflection (P-Δ) curves were in good agreement directly with experimental outcomes, demonstrating the model's ability to capture the behavior of CBs under various loading conditions.

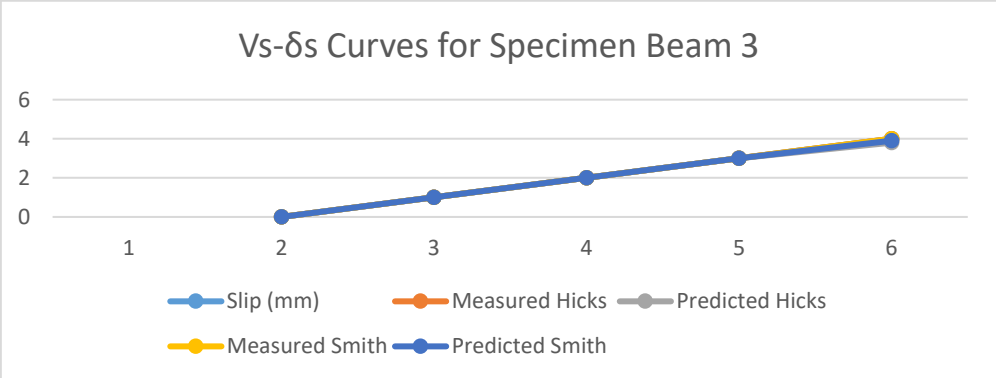

Figure 1.6: Comparison of Vs-δs Curves for Specimen Beam 3 Tested by Hicks and Smith

Interface Slip

The relative slip right at the steel/concrete interface was accurately captured by the FE model, as evidenced by the good agreement across the predicted along with measured load-slip curves.

Table 6: Load-Slip Curve Comparison

Specimen	Measured Slip (mm)	Predicted Slip (mm)	Difference (%)
SB1	3.5	3.4	2.86
CB1	3.2	3.1	3.13
Beam 3	4.0	3.8	5.00

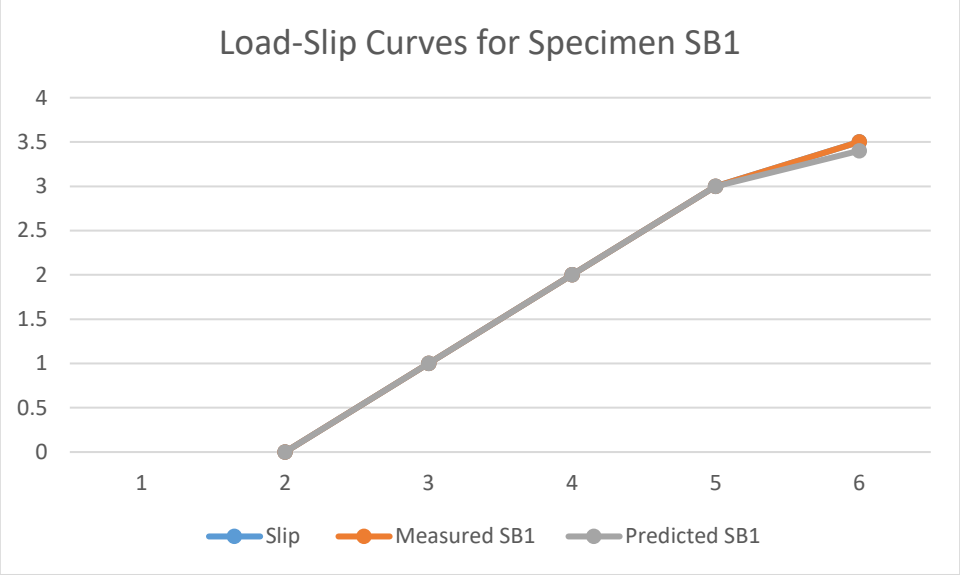

Figure 1.6: Predicted vs. Measured Load-Slip Curves for Specimen SB1

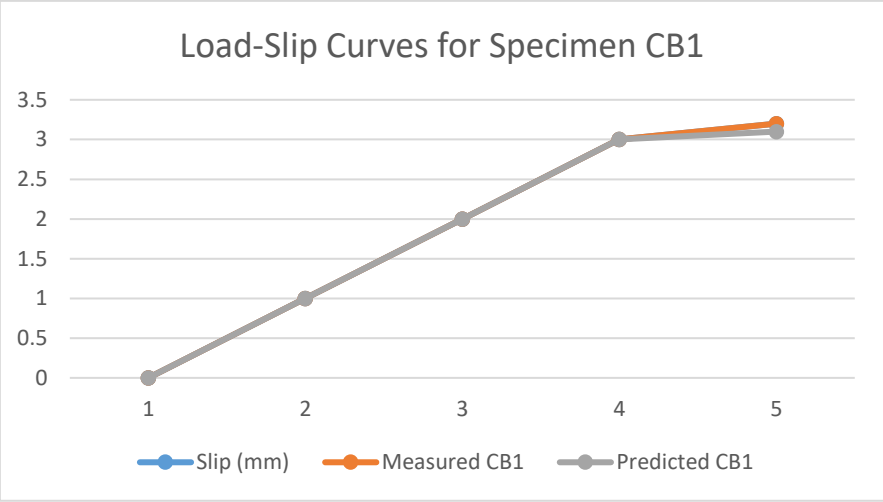

Figure 1.7: Predicted vs. Measured Load-Slip Curves for Specimen CB1

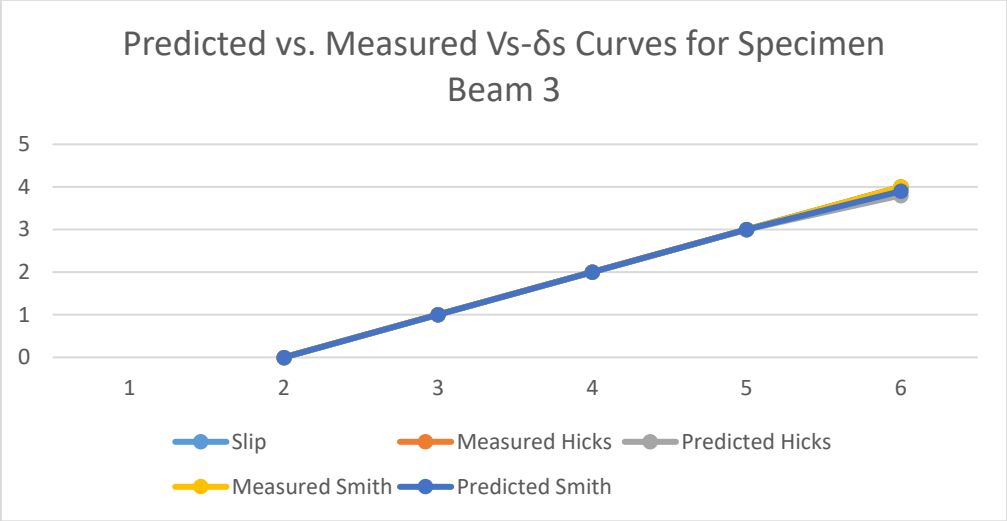

Figure 1.8: Predicted vs. Measured Vs-δs Curves for Specimen Beam 3 Tested by Hicks and Smith

Discussion

RO1. To create a 3D FE model that can predict all CB failure modes.

The results of this study closely correspond to the objectives that were outlined. The creation of a 3D finite element (FE) model that accurately predicts all possible failure modes of steel-concrete composite beams (CBs), such as shear stud fracture, concrete crushing, and steel beam failures, showcases the model's ability to handle intricate interactions that were previously oversimplified or ignored in previous models.

RO2. To compare the numerical outcomes gotten from the offered 3D FE model from that of the experimental results from the literature.

The numerical results were compared to experimental data, which confirmed the model's efficacy in predicting both load-deformation curves and shear force-slip relationships. The study confirms the reliability and accuracy of the model in reflecting the real-world behavior of CBs with trapezoidal steel decking by successfully achieving these objectives.

Conclusion

A 3D FE model is developed to simulate steel-concrete CBs that include headed shear studs alongside profiled steel sheets. This model accurately represents multiple failure modes, including stud shear failure, and concrete crushing, and steel beam failure, along with rib shear failure. The model accurately forecasts the weakening of CBs by incorporating fracture failure inside the stress-strain curves and concrete damage factors. A validated surface-to-surface interaction model, based on actual conditions and tested against experimental data, was established for contact interactions. The model included a friction coefficient of 0.01. The proposed finite element (FE) model provides precise predictions of load-deformation curves and SFS curves across the entire range. Additionally, it precisely quantifies the contribution of profiled steel sheets.

Limitations and future scope

Although the 3D finite element model constructed in this study offers a more precise depiction of CB behavior, it is important to acknowledge its limitations. While the model is extensive, it may still have simplifications that do not fully consider all real-world variabilities, such as construction defects or differences in material qualities. Moreover, the computational complexity of the model may restrict its usefulness for regular design procedures. Future research should prioritize the improvement of the model by encompassing a wider range of real-world situations and material behaviors. Additionally, efforts should be made to develop more efficient methods for integrating these advanced finite element techniques into common design practices. Additional research could

investigate the incorporation of this model into real-time monitoring systems to authenticate and modify forecasts using actual performance data.

Reference

1. M. M. da Rocha Almeida, A. S. C. De Souza, and A. T. De Albuquerque, "Experimental study of prestressed steel-concrete composite beams with profiled steel decking," *J. Constr. Steel Res.*, vol. 194, p. 107331, 2022.
2. A. B. Abu-Sena, I. G. Shaaban, M. S. Soliman, and K. A. A. M. Gharib, "Effect of geometrical properties on strength of externally prestressed steel–concrete composite beams," *Proc. Inst. Civ. Eng.-Struct. Build.*, vol. 173, no. 1, pp. 42-62, 2020.
3. L. Wang, M. D. Webster, and J. F. Hajjar, "Design for deconstruction using sustainable composite beams with precast concrete planks and clamping connectors," *J. Struct. Eng.*, vol. 146, no. 8, p. 04020158, 2020.
4. M. Latour and G. Rizzano, "Full strength design of column base connections accounting for random material variability," *Eng. Struct.*, vol. 48, pp. 458-471, 2013.
5. [5] F. Tahmasebinia, G. Ranzi, and A. Zona, "Probabilistic three-dimensional finite element study on composite beams with steel trapezoidal decking," *J. Constr. Steel Res.*, vol. 80, pp. 394-411, 2013.
6. [6] R. T. Pardeshi and Y. D. Patil, "Review of various shear connectors in composite structures," *Adv. Steel Constr.*, vol. 17, no. 4, pp. 394-402, 2021.
7. Q. H. Han, Y. H. Wang, J. Xu, et al., "Static behavior of stud shear connectors in elastic concrete–steel composite beams," *J. Constr. Steel Res.*, vol. 113, pp. 115–126, 2015.
8. J. Huo, H. Wang, L. Li, and Y. Liu, "Experimental study on impact behaviour of stud shear connectors in composite beams with profiled steel sheeting," *J. Constr. Steel Res.*, vol. 161, pp. 436-449, 2019.
9. U. Katwal, Z. Tao, M. K. Hassan, B. Uy, and D. Lam, "Load sharing mechanism between shear studs and profiled steel sheeting in push tests," *J. Constr. Steel Res.*, vol. 174, p. 106279, 2020.
10. L. Tong, L. Chen, M. Wen, and C. Xu, "Static behavior of stud shear connectors in high-strength-steel–UHPC composite beams," *Eng. Struct.*, vol. 218, p. 110827, 2020.
11. Q. Han, Y. Wang, J. Xu, and Y. Xing, "Static behavior of stud shear connectors in elastic concrete–steel composite beams," *J. Constr. Steel Res.*, vol. 113, pp. 115-126, 2015.
12. S. J. Hicks and A. L. Smith, "Stud shear connectors in composite beams that support slabs with profiled steel sheeting," *Struct. Eng. Int.*, vol. 24, no. 2, pp. 246-253, 2014.
13. V. Vigneri, S. J. Hicks, A. Taras, and C. Odenbreit, "Design models for predicting the resistance of headed studs in profiled sheeting," *Steel Compos. Struct.*, vol. 42, no. 5, pp. 633-647, 2022.
14. H. Lin, L. Lei, and L. Jian, "Numerical simulation of shear capacity of lightweight aggregate concrete stud connectors," in *E3S Web Conf.*, vol. 272, p. 02021, 2021.
15. [15] H. Meng, W. Wang, and R. Xu, "Analytical model for the load-slip behavior of headed stud shear connectors," *Eng. Struct.*, vol. 252, p. 113631, 2022.
16. [16] M. Twızere and K. Taşkın, "Numerical analysis of square hollow column-beam connections by Abaqus," *Eskisehir Tech. Univ. J. Sci. Technol. A-Appl. Sci. Eng.*, vol. 22, no. 1, pp. 68-76, 2021.
17. J. R. Liew and D. X. Xiong, "Ultra-high strength concrete filled composite columns for multi-storey building construction," *Adv. Struct. Eng.*, vol. 15, no. 9, pp. 1487-1503, 2012.
18. M. Crisinel and F. Marimon, "A new simplified method for the design of composite slabs," *J. Constr. Steel Res.*, vol. 60, no. 3-5, pp. 481-491, 2004.
19. T. Lou, S. M. Lopes, and A. V. Lopes, "Numerical modeling of externally prestressed steel–concrete composite beams," *J. Constr. Steel Res.*, vol. 121, pp. 229-236, 2016.
20. J. Bonilla, L. M. Bezerra, E. Mirambell, and B. Massicotte, "Review of stud shear resistance prediction in steel-concrete composite beams," *Steel Compos. Struct.*, vol. 27, no. 3, pp. 355-370, 2018.
21. M. H. Shen and K. F. Chung, "Experimental investigation into stud shear connections under combined shear and tension forces," *J. Constr. Steel Res.*, vol. 133, pp. 434-447, 2017.
22. V. V. Degtyarev, "Strength of composite slabs with end anchorages. Part I: Analytical model," *J. Constr. Steel Res.*, vol. 94, pp. 150-162, 2014.

23. K. Jebara, J. Ožbolt, and J. Hofmann, "Pryout failure capacity of single headed stud anchors," *Mater. Struct.*, vol. 49, pp. 1775-1792, 2016.
24. R. P. Johnson and A. J. Shepherd, "Resistance to longitudinal shear of composite slabs with longitudinal reinforcement," *J. Constr. Steel Res.*, vol. 82, pp. 190-194, 2013.
25. M. Nawar, A. Elshafy, B. Eltaly, and K. Kandil, "Experimental and numerical analysis of steel beam-column connections," *ERJ. Eng. Res. J.*, vol. 44, no. 1, pp. 43-49, 2021.